Functional characterization of genes mediating cell wall metabolism and responses to plant cell wall integrity impairment

Timo Engelsdorf[1, 2], Lars Kjaer[3, 4], Nora Gigli-Bisceglia[1, 5], Lauri Vaahtera[1], Stefan Bauer[6, 7], Eva Miedes[8, 9], Alexandra Wormit[3, 10], Lucinda James[3, 11], Issariya Chairam[3, 11], Antonio Molina[8, 9] and Thorsten Hamann[1, 3]*

[1]Institute for Biology, Faculty of Natural Sciences, Norwegian University of Science and Technology, 5 Høgskoleringen, Trondheim, 7491, Norway.

[2] Present address: Division of Plant Physiology, Department of Biology, Philipps University of Marburg, 35043 Marburg, Germany.

[3] Division of Cell and Molecular Biology, Department of Life Sciences, Imperial College London, Sir Alexander Fleming Building, South Kensington Campus, London, SW72AZ, UK.

[4] Present address: Sjælland erhvervsakademi, Breddahlsgade 1b, 4200 Slagelse, Zealand, Denmark

[5] Present address: Laboratory of Plant Physiology, 6708PB Wageningen University and Research, Wageningen, the Netherlands.

[6] Energy Biosciences Institute, University of California, 120A Energy Biosciences Building, 2151 Berkeley Way, MC 5230, Berkeley, CA 94720-5230

[7] Present address: Zymergen, Inc. 5980 Horton St, Suite 105 Emeryville, CA 94608, USA

[8] Centro de Biotecnología y Genómica de Plantas, Universidad Politécnica de Madrid (UPM)- Instituto Nacional de Investigación y Tecnología Agraria y Alimentaria (INIA), Campus de Montegancedo-UPM, 28223 Pozuelo de Alarcón, Madrid, Spain.

[9] Departamento de Biotecnología-Biología Vegetal, Escuela Técnica Superior de Ingeniería Agronómica, Alimentaria y de Biosistemas, Universidad Politécnica de Madrid (UPM), 28040 Madrid, Spain.

[10] Present address: RWTH Aachen, Institute for Biology I, Worringerweg 3, D-52056 Aachen, Germany.

[11] Present address: ADAS, Battlegate Road, Boxworth, Cambridge, CB23 4NN, UK.

[12] Present address: Department of Nuclear Safety and Security, International Atomic Energy Agency, Vienna International Centre, PO Box 100, 1400 Vienna, Austria.

* For correspondence: Tel. +47 91825937 E-mail: Thorsten.hamann@ntnu.no

Funding

This work was supported through Gatsby AdHoc funds and a grant from the Peder Sather Center for Advanced Study to T.H. and Chris Somerville. L.K. was supported by a Ph.D. Fellowship from the Porter Institute at Imperial College and I.C. by a PhD fellowship provided by the Royal Thai government. L.D. and A.W were supported through postdoctoral fellowships provided by the Porter Institute at Imperial College. T.E. was supported through a EU Marie Curie Fellowship "SUGAROSMO-SIGNALLING" and a DFG postdoctoral fellowship (EN 1071/1-1). N.G. was supported through the EEA project grant CYTOWALL. Research by A.M. was supported by Spanish Ministry of Economy and Competitiveness (MINECO) grant BIO2015-64077-R.

Abstract

Plant cell walls participate in all plant-environment interactions. Maintaining cell wall integrity (CWI) during these interactions is essential. This realization led to increased interest in CWI and resulted in knowledge regarding early perception and signalling mechanisms active during CWI maintenance. By contrast, knowledge regarding processes mediating changes in cell wall metabolism upon CWI impairment is very limited. To identify genes involved and to investigate their contributions to the processes we selected 23 genes with altered expression in response to CWI impairment and characterized the impact of T-DNA insertions in these genes on cell wall composition using Fourier-Transform Infrared Spectroscopy (FTIR) in *Arabidopsis thaliana* seedlings. Insertions in 14 genes led to cell wall phenotypes detectable by FTIR. A detailed analysis of four genes found that their altered expression upon CWI impairment is dependent on THE1 activity, a key component of CWI maintenance. Phenotypic characterizations of insertion lines suggest that the four genes are required for particular aspects of CWI maintenance, cell wall composition or resistance to *Plectosphaerella cucumerina* infection in adult plants. Taken together, the results implicate the genes in responses to CWI impairment, cell wall metabolism and/or pathogen defence, thus identifying new molecular components and processes relevant for CWI maintenance.

Keywords: Cell wall, cell wall integrity**,** cell wall metabolism, cell wall signalling, plant pathogen-interaction.

Acknowledgments

Programming support from Ane-Kjersti Vie and help with lignin and phytohormone quantification from Trude Johansen and the PROMEC facility at NTNU are gratefully acknowledged.

Introduction

Plant cell walls are involved in all interactions between plants and their environment. Examples include pathogen infection or exposure to drought, where wall composition and structure change to prevent water loss, pathogen susceptibility or at least limit further pathogen spread (Bacete et al., 2018; Novaković et al., 2018). These changes of the walls are exemplified by reinforcement with callose during infection or modifications of pectic polysaccharides to prevent water loss during exposure to drought stress (Chowdhury et al., 2016; Dinakar & Bartels, 2013). Cell walls are extremely plastic, undergoing dynamic changes to enable plant cells to expand and differentiate during growth and development (Bidhendi & Geitmann, 2015). Controlled deposition of cellulose microfibrils through interactions between cellulose synthases and microtubules during cell expansion exemplify the changes in cell wall organization, permitting tightly controlled cell expansion (Gutierrez et al., 2009; Paredez et al., 2006). Deposition of suberin and lignin during formation of the casparian strip in pericycle cells of the primary root exemplifies modifications of cell walls during cell differentiation (Barbosa et al., 2019; Doblas et al., 2017; Lee et al., 2013). These examples illustrate processes active during plant-environment interactions and development, enabling cell walls to fulfill their respective biological functions.

How do cell walls perform these various functions, which sometimes involve opposite performance requirements, while simultaneously maintaining their functional integrity? The available evidence supports the existence of a dedicated mechanism, which is monitoring the functional integrity of the plant cell wall and initiates adaptive changes in cellular and cell wall metabolism to maintain cell wall integrity (CWI) (De Lorenzo et al., 2018; Doblas et al., 2018; Hamann, 2015; Kieber & Polko, 2019; Wolf, 2017). Studies of the mode of action of the CWI maintenance mechanism often investigate the responses to cell wall damage (CWD), which can be generated by cell wall degrading enzymes (cellulase, pectinase etc.) or compounds like isoxaben (ISX) (Engelsdorf et al., 2018). ISX inhibits specifically cellulose production during

primary cell wall formation in elongating plant cells (Heim et al., 1990; Scheible et al., 2001; Tateno, Brabham, & DeBolt, 2016). Established responses to CWD include growth inhibition involving cell cycle arrest, changes in the levels of phytohormones like jasmonic acid (JA), salicylic acid (SA) and cytokinins (CKs) as well as changes in cell wall composition involving pectic polysaccharides, lignin and callose deposition (Cano-Delgado et al., 2003; Denness et al., 2011; Ellis & Turner, 2001; Gigli-Bisceglia et al., 2018; Manfield et al., 2004).

The available evidence implicates receptor-like kinases (RLK) like MALE DISCOVERER 1-INTERACTING RECEPTOR LIKE KINASE 2 (MIK2), FEI1, FEI2, THESEUS 1 (THE1) and FERONIA (FER) in CWI maintenance (Engelsdorf et al., 2018; Feng et al., 2018; Hematy et al., 2007; Van der Does et al., 2017; Xu et al., 2008). THE1 and FER belong to the *Catharanthus roseus* RLK1-like kinase (*Cr*RLK1L) family, which has 17 members. These RLKs consist of an intracellular Serine / Threonine-kinase domain, a transmembrane domain and an extracellular domain exhibiting similarity to the malectin domain originally identified in *Xenopus laevis* (Franck et al., 2018). Currently it is not clear if malectin domains in *Cr*RLK1Ls are either required for binding to cell wall epitopes, mediate protein-protein interaction or actually do both (Du et al., 2018; Feng et al., 2018; Gonneau et al., 2018; Haruta et al., 2018; Moussu et al., 2018; Stegmann et al., 2017). FER is required during gametophytic and root hair development, salt stress, JA signaling and coordination between abscisic acid- (ABA) and JA-based signaling processes (Duan et al., 2010; Escobar-Restrepo et al., 2007; Feng et al., 2018; Guo et al., 2018; Kanaoka & Torii, 2010; Shih et al., 2014; Yu et al., 2012; Zhao et al., 2018). MIK2 and THE1 are required for root development, CWD-induced lignin and phytohormone production as well as resistance to the root pathogen *Fusarium oxysporum* (Engelsdorf et al., 2018; Gonneau et al., 2018; Hematy et al., 2007; Van der Does et al., 2017). FEI1 and FEI2 have been originally identified through their impact on seedling root growth on medium containing 4.5% sucrose and subsequently implicated in a cell wall signaling pathway involving the SALT OVERLY SENSITIVE5 (SOS5) and FEI2 (Harpaz-Saad et al., 2011; Shi

et al., 2003; Xue et al., 2017). In parallel, ion-channels, like MID1-COMPLEMENTING ACTIVITY 1 (MCA1) and MECHANOSENSITIVE CHANNEL OF SMALL CONDUCTANCE-LIKE 2 (MSL2) and 3 (MSL3) were shown to contribute to activation of CWD-induced responses in plants (Denness et al., 2011; Engelsdorf et al., 2018). MCA1 was originally identified through its´ ability to partially complement a MID1/CCH1- deficient *Saccharomyces cerevisiae* strain (Nakagawa et al., 2007). In yeast MID1/CCH1 form a plasmamembrane-localized stretch-activated calcium channel required both for mechano-perception and CWI maintenance (Levin, 2011). CWD-induced responses in plants (like in yeast cells) seem also to be sensitive to turgor manipulation (Hamann, 2015; Levin, 2011). The reason being that in *Arabidopsis thaliana* seedlings, exposed simultaneously to ISX and mild hyperosmotic conditions, most of the CWD-induced responses are suppressed in a concentration dependent manner (Engelsdorf et al., 2018; Hamann et al., 2009). The early signals generated seem to be conveyed to downstream response mediators through changes in production of reactive oxygen species (ROS) and phytohormones (JA/SA/CKs) (Denness et al., 2011; Gigli-Bisceglia et al., 2018). Enzymes implicated in ROS production upon CWI impairment are NADPH-oxidases like RESPIRATORY BURST OXIDASE HOMOLOGUE (RBOH) D/F (after ISX-treatment) or RBOH H/J during pollen tube development (Jiménez-Quesada et al., 2016). NADPH-oxidase activity in turn can be regulated via calcium binding, differential phosphorylation involving kinases controlled by changes in calcium levels (CALCINEURIN INTERACTING KINASE 26, CIPK26), activated in response to pathogen infection through phosphorylation involving BOTRYTIS INDUCED KINASE 1 (BIK1) or controlled via RHO GTPases, a ROPGEF and FER (Duan et al., 2010; Han et al., 2018; Kadota et al., 2014).

This abbreviated overview of molecular components active during plant CWI maintenance illustrates the increase in knowledge regarding putative CWI sensors and early signal transduction elements in recent years. Whilst it is fascinating to know about early CWD

166 perception and signaling processes we also need to understand how signals generated lead to
167 changes in cell wall composition and structure to dissect the mode of action of the CWI
168 maintenance mechanism thoroughly. This is of particular interest in the context of targeted
169 modification of biomass quality and improvement of food crop performance since the CWI
170 maintenance mechanism seems to be an important component of cell wall plasticity (Doblin et
171 al., 2014; Mahon & Mansfield, 2019). Cell wall plasticity in turn has been discussed as the root
172 cause for the apparently limited success of efforts aimed at optimizing biomass quality that
173 have been achieved so far (Doblin et al., 2014).

174 We wanted to identify additional components and molecular processes, which are
175 mediating responses to CWD and adaptive changes in cell wall metabolism. To achieve these
176 aims we selected candidate genes using microarray-based expression profiling data deriving
177 from ISX-treated Arabidopsis seedlings. Fourier Transform Infrared (FTIR) Spectroscopy was
178 then used to identify candidate genes where insertions lead to cell wall changes on the seedling
179 level. We performed in depth studies for four genes to validate the approach. These studies
180 involved confirming that gene expression is responsive to ISX, determining if expression is
181 controlled by THE1 and investigating how loss of function alleles for these genes affect cell
182 wall composition in adult plants, resistance to the necrotrophic pathogen *Plectosphaerella*
183 *cucumerina* and responses to ISX-induced CWD impairing CWI.

Materials and Methods

Reagents

All chemicals and enzymes were purchased from Sigma-Aldrich unless stated otherwise.

Plant Material

Wild-type and mutant *Arabidopsis thaliana* lines used in this study were ordered from the Nottingham Arabidopsis Stock Centre (http://arabidopsis.info/). Detailed information is listed in Supplemental Table S1. Seedlings were grown for 6 days in liquid culture (2.1 g/L Murashige and Skoog Basal Medium, 0.5 g/L MES salt and 1 % sucrose at pH 5.7) before treatment with 600 nM isoxaben (in DMSO) as described (Engelsdorf et al., 2018). For cell wall analysis, plants were grown on soil (Pro-Mix HP) in long-day conditions (16 h light, 11000 Lux, 22°C; 8 h dark, 20 °C; 70 % relative humidity). For pathogen infection assays, plants were grown in phytochambers on sterile soil-vermiculite (3:1) under short-day conditions (10 h of light/14 h of dark) at 20-21 ºC.

Pathogen Infection Assays

For *Plectosphaerella cucumerina* BMM (*Pc*BMM) pathogenicity assays, 18 days-old plants (n >15) were sprayed with a spore suspension (4 x 10^6 spores/ml) of the fungus as previously described (Delgado-Cerezo et al., 2011; Sanchez-Vallet et al., 2010). Fungal biomass *in planta* was quantified by determining the level of the *Pc*BMM β-tubulin gene by qPCR (forward primer: CAAGTATGTTCCCCGAGCCGT and reverse primer: GGTCCCTTCGGTCAGCTCTTC) and normalizing these values to those of *UBIQUITIN-CONJUGATING ENZYME21* (*UBC21*, *AT5G25760*).

Quantitative RT-PCR

Total RNA was isolated using a Spectrum Plant Total RNA Kit (Sigma-Aldrich). Two micrograms of total RNA were treated with RQ1 RNase-Free DNase (Promega) and processed with the ImProm-II Reverse Transcription System (Promega) for cDNA synthesis. qRT-PCR was performed with a Roche LightCycler 480 system using LightCycler 480 SYBR Green I Master. Gene expression levels were determined as described (Gigli-Bisceglia et al., 2018). The following gene-specific primers have been used for time course expression analysis in Col-0:

ACT2-FOR (5'-CTTGCACCAAGCAGCATGAA-3'),

ACT2-REV (5'-CCGATCCAGACACTGTACTTCCTT-3'),

WSR1-FOR (5'-TATGGTGATGAACTTTGCGTTC-3'),

WSR1-REV (5'-ACTCAACAGTAGCATCTCCTGA-3'),

WSR1A-FOR (5'-TACGCTGCTACTGGTCAACG-3'),

WSR1A-REV (5'-TTCCTCCAATCACCGGCATC-3'),

WSR2-FOR (5'-CTCACTTCCATCGTTTCAAGTG-3'),

WSR2-REV (5'-GAAACCAAACGTGGCCTAAA-3'),

WSR3-FOR (5'-GAAAGCACGAGACTGGAACG-3'),

WSR3-REV (5'-TATCCACCCTCCAACGCAAA-3'),

WSR4-FOR (5'-AGCCCTGAGAGATCAAGCATT-3'),

WSR4-REV (5'-AGCTCAACTAAGCGATGAAGC-3').

For the characterization of T-DNA insertion lines, the following primers have been employed:

ACT2-FOR, ACT2-REV, WSR1-FOR, *WSR1-REV*, *WSR2-FOR*, *WSR2-REV*, *WSR3-FOR2* (5'-TCTTATCCGGTTGCGGAAGG-3'),

WSR3-REV2 (5'-GTGGTGAGATGACCCAGAGC-3'),

WSR4-FOR2 (5'-CTTGATGCAGTTGTGAAAGCA-3'),

WSR4-REV2 (5'-TCTTCACCGAAACAATCATCC-3').

FTIR Spectroscopy and Analysis

For FTIR analysis, 4 biological replicates per genotype and 5 technical replicates per biological replicate were collected (i.e. for each genotype 20 spectra were collected). Spectra for each technical replicate were measured from 800 to 5000 cm^{-1} with 15 accumulations per measurement on a Bruker Vertex 70. All spectra were measured at 10 kHz, with a 10 kHz lowpass filter and the Fourier transform was carried out using Blackman-Harris 3-term. Atmospheric compensation was carried out on the data using OPUS version 5 (www.bruker.com). The spectra were cropped to the area between 802 cm^{-1} to 1820 cm^{-1} to cover informative wavenumbers as described in (Mouille et al., 2003). Linear regression was carried out based on the first ten points in either end of the spectra and used for baseline correction. The data was normalized to sum 1 with any negative values still present set to 0 for normalization purposes. Biological variation in the Col-0 controls was determined based on three independent experiments carried out with 4 biological replicates and 5 technical replicates per biological replicate (i.e. 20 spectra per experiment). The difference between the insertion lines and Col-0 was calculated by averaging all the technical repeats for a line and subtracting the corresponding average from Col-0. The difference between the insertion lines and Col-0 was plotted by wavelength. Two times the standard deviation of Col-0 was chosen as a cutoff as it would indicate significance if the natural variation is assumed to be symmetrical across Col-0 and the insertion line.

Cell Wall Analysis

Cell wall preparation and analysis were performed as described (Yeats et al., 2016) with minor modifications. For analysis of stem cell wall composition, major stems of three plants per genotype were pooled to form one biological replicate. For analysis of leaf cell wall composition, whole leaf rosettes of three plants per genotype were pooled to form one biological replicate. Four biological replicates were analysed in all cases. Plant samples were

262 immediately flash-frozen in liquid nitrogen after sampling and lyophilized. Dried material was
263 ball-milled with zirconia beads in a Labman robot (www.labmanautomation.com), extracted
264 three times with 70 % ethanol at 70°C and dried under vacuum. Starch was removed using a
265 Megazyme Total Starch Kit according to the manufacturer's instructions. After drying under
266 vacuum, de-starched alcohol insoluble residue (AIR) was weighed out in 2 ml screw caps tubes
267 for cell wall monosaccharide analysis (2 mg AIR) and GC vials for lignin analysis (1.2 mg
268 AIR), respectively, with the Labman robot (0.2 mg tolerance). Cellulose, neutral sugars and
269 uronic acids were determined following the published one-step two-step hydrolysis protocol
270 (Yeats et al., 2016). High-performance anion-exchange chromatography with pulsed
271 amperometric detection (HPAEC-PAD) was performed on a Thermo Fisher Dionex ICS-3000
272 system with CarboPac PA-20 and PA-200 columns as described (Yeats et al., 2016). Acetyl
273 bromide soluble lignin was quantified as described (Chang et al., 2008)
274
275 *Phytohormone Analysis*
276 JA and SA were extracted and analysed as described (Engelsdorf et al., 2018). Briefly,
277 extraction was performed in 10 % methanol / 1 % acetic acid with Jasmonic-d_5 Acid and
278 Salicylic-d_4 Acid (CDN Isotopes) as internal standards. Quantification was performed on a
279 Shimadzu UFLC XR / AB SCIEX Triple Quad 5500 system using the following mass
280 transitions: JA 209 > 59, D_5-JA 214 > 62, SA 137 > 93, D_4-SA 141 > 97.
281
282 *Lignin Detection in Roots*
283 Lignification in seedling roots (n>15) was analysed 24 h after start of treatment.
284 Lignified regions were detected with phloroglucinol-HCL, photographed with a Zeiss Axio
285 Zoom.V16 stereomicroscope and quantified as described (Engelsdorf et al., 2018).
286
287

288 *Statistical Analysis*

289 Statistical significance was assessed using Student's *t*-test in Microsoft Excel (2-tailed
290 distribution, two-sample unequal variance). Statistically significant differences are indicated by
291 * $p < 0.05$, * $p < 0.01$. Boxplots were generated using R package "boxplot" with default settings
292 (range = 1.5*IQR).

293

294

295 **Results**

296 **Identification of candidate genes**

297 Previously, we have performed time course experiments to characterize the response of
298 Arabidopsis seedlings to ISX-induced CWD (Hamann et al., 2009). Affymetrix ATH1
299 microarrays were used to detect changes in transcript levels up to 36 hours after start of ISX
300 treatment. The phenotypic characterization of seedlings detected lignin deposition in root tips
301 and enhanced JA production after 4-6 hours of ISX-treatment (Hamann et al., 2009). Based on
302 these results we hypothesized that genes exhibiting transcriptional changes after 4 hours might
303 be involved in CWD responses (phytohormone and lignin production) as well as cell wall
304 modifying processes in general. Analysis of the microarray derived expression data suggested
305 that the transcript levels of several hundred genes change after 4 hours of exposure to ISX. We
306 used public expression data (www.genevestigator.com) to identify genes exhibiting differential
307 expression after 4 hours of ISX treatment and elevated expression in tissue types where cell
308 wall modification or production occurs preferentially (primary root elongation zone and
309 expanding hypocotyl). To determine whether these candidates are involved in cell wall related
310 processes, we decided to perform a pilot study characterizing the phenotypes of T-DNA
311 insertion lines for 23 candidate genes. Supporting information Table 1 (Table S1) lists the 23
312 candidate genes with their database annotations, the probe sets representing the genes on the
313 Affymetrix ATH1 microarray and insertion lines used for characterization. Figure S1

314 summarizes the microarray-derived expression data for the 23 candidate genes generated in the
315 original time course expression profiling experiments. The genes are separated based on their
316 transcript levels either being apparently increased (Figure S1a) or decreased (Figure S1b) over
317 time. Figure S2 illustrates the putative transcript levels of the candidate genes in different
318 tissues / organs. The genevestigator-derived expression data suggest that several candidate
319 genes are involved in cellular and biological processes, which affect or involve plant cell wall
320 metabolism.
321
322 **FTIR-based analysis detects cell wall phenotypes in mutant seedlings**
323 Performing detailed cell wall analysis for insertion lines in 23 candidate genes would be
324 time consuming and possibly not very efficient. Previously, FTIR has been successfully used
325 as an efficient approach to classify *Arabidopsis* mutants with altered cell wall architecture
326 (Mouille et al., 2003). We used this approach as foundation to facilitate identification of
327 insertions in candidate genes leading to changes in cell wall composition or structure in
328 Arabidopsis seedlings. FTIR spectra were collected for analysis from total cell wall material
329 derived from 6 days-old, liquid culture grown Col-0 seedlings or seedlings with T-DNA
330 insertions in the candidate genes. Initially only Col-0 samples were characterized to establish
331 the variability observed in controls. Subsequently, twice the standard deviation of the Col-0
332 variability was used as a cut-off to identify insertions in candidate genes causing significant
333 changes in the FTIR spectra. Based on this criterium FTIR spectra for 14 of the 23 insertion
334 lines analyzed exhibited significant differences (Figure S3). Pronounced differences were
335 observed for insertions in *At5g24140* (*SQUALENE MONOOXYGENASE2*, *SQP2)* and
336 *At5g49360* (*BETA-XYLOSIDASE1, ATBXL1*) in the 1700-1600 cm^{-1} (pectin ester, carboxylate
337 / carbonyl side groups) and 1200-950 cm^{-1} (characteristic for cellulose and elements of pectic
338 polysaccharides) areas (Figure S3, blue rectangle) (Arsovski et al., 2009; Rasbery et al., 2007;
339 Szymanska-Chargot et al.,. Insertion lines for *At2g41820* (*PHLOEM INTERCALATED WITH*

XYLEM / TRACHEARY ELEMENT DIFFERENTIATION INHIBITORY FACTOR RECEPTOR-CORRELATED 3, PXC3), *At3g11340 (UDP GLYCOSYLTRANSFERASE 76B1*, *UGT76B1*), *At4g33420* (*PEROXIDASE 47*, *PRX47*), *At4g35630* (*PHOSPHOSERINE AMINO-TRANSFERASE 1*, *PSAT 1*), *At5g48460* (*FIMBRIN 2, ATFIM2*), *At5g47730* (*SEC14-HOMOLOGUE 19*, *SFH19*) and *At5g65390* (*ARABINOGALACTAN PROTEIN 7*, *AGP7*) exhibited differences in the 1367-1200 cm^{-1} area typical for certain cellulose elements, hemicelluloses and pectins (Figure S3, red rectangles) (Maksym et al., 2018; Seifert, 2018; Szymanska-Chargot et al., 2015; Tokunaga et al., 2009; Wang et al., 2013; Wulfert & Krueger, 2018; Zhang et al., 2016). In the 1200-950 cm^{-1} area distinctive differences were detected for insertion lines in five candidate genes *At1g07260* (*UGT71C3*), *At1g74440*, *At2g35730*, *At3g13650 (DIRIGENT PROTEIN 7*, *DIR7)* and *At4g33300* (*ACTIVATED DISEASE RESISTANCE-LIKE 1*, *ADR1-L1*) (Figure S3, purple rectangles) (Dong et al., 2016; Meier et al., 2008; Paniagua et al., 2017; Rehman et al., 2018; Wuest et al., 2010). The results from the FTIR-based analysis of the insertion lines suggested that cell wall composition or structure is affected in seedlings with insertions for 14 of the 23 candidate genes examined. The insertions seemed to have distinct effects on cell wall composition / structure based on their apparent separation into three groups.

Four candidate genes are selected for more detailed characterization

We selected four candidate genes for a more detailed analysis (*At3g13650*, *At2g35730*, *At5g47730* and *At2g41820*, Table 1) because of the limited knowledge available regarding their biological functions and the four insertions leading to two qualitatively different FTIR phenotypes. This enabled us to determine also if insertion lines resulting in similar FTIR cell wall phenotypes on the seedling level exhibit similar cell wall phenotypes on the adult plant level. While *At3g13650* and *At2g35730* FTIR-spectra (orange, yellow) seemed to deviate from Col-0 controls mainly in areas characteristic for cellulose and certain types of pectins,

366 *At5g47730* and *At2g41820* spectra (green, blue) deviated mainly in areas characteristic for
367 cellulose elements, hemicelluloses and pectins (Figure 1, numbers highlight wavenumbers
368 diagnostic for certain bands in the spectra according to Szymanska-Chargot et al., 2015). These
369 four genes were classified as WALL STRESS RESPONSE genes or WSRs. *At3g13650* (*WSR1,*
370 *DIR7*) belongs to a family of disease resistance responsive proteins, which have been implicated
371 in lignan biosynthesis and formation of the casparian strip (Barbosa et al., 2019; Paniagua et
372 al., 2017). Analysis of the available data suggests that *At2g35730* (*WSR2*) is expressed in the
373 female gametophyte and encodes a heavy metal transport / detoxification superfamily protein
374 (De Abreu-Neto et al., 2013; Wuest et al., 2010). Protein homology suggests that *At5g47730*
375 (*WSR3, SFH19*) is related to SEC14 proteins from *S. cerevisiae*, which have been implicated in
376 polarized vesicle transport (KF de Campos & Schaaf, 2017). *At2g41820* (*WSR4, PXC3*)
377 encodes a putative leucine-rich repeat receptor kinase, belonging to a family where other
378 members have been implicated in organization of secondary vascular tissue (Wang et al., 2013).
379
380 **Quantitative gene expression analysis confirms transcriptomics results and suggests**
381 **THE1 is controlling *WSR* gene expression**
382 DNA microarray-based expression analysis of Arabidopsis seedlings suggested that the
383 transcript levels of the *WSR* genes are changing in response to ISX treatment (Figure S1). To
384 confirm this, we performed time course experiments and transcript levels of the four genes were
385 determined through quantitative reverse transcription – polymerase chain reaction (qRT - PCR)
386 in mock- or ISX-treated seedlings. The transcript levels of *WSR1, 2* and *3* increased after 4
387 hours of ISX treatment and remained elevated compared to mock controls (Figure 2a).
388 Transcript levels of *WSR4* were reduced after an initial transient increase. To establish if
389 expression of the *WSR* genes is controlled by the THE1-mediated CWI maintenance mechanism
390 we investigated *WSR* transcript levels in THE1 loss (*the1-1*) - or gain-of-function (*the1-4*)
391 seedlings (Hematy et al., 2007; Merz et al., 2017). In ISX-treated Col-0 seedlings *WSR1*, *2* and

392 *3* transcript levels were increased while *WSR4* seemed slightly reduced after eight hours (Figure
393 2b). *WSR1* transcript levels were not increased in *the1-1* seedlings but the increase was
394 enhanced in *the1-4*. *WSR2* transcript levels changed in *the1-1* seedlings as in Col-0 while the
395 increase was enhanced in *the1-4*. Increases in *WSR3* expression were apparently slightly
396 reduced in *the1-1* seedlings compared to Col-0 while the increase was again more pronounced
397 in *the1-4* than in ISX-treated Col-0 seedlings. Decrease of *WSR4* expression seemed absent in
398 *the1-1* compared to ISX-treated Col-0 seedlings and was enhanced in ISX-treated *the1-4*
399 seedlings. In conclusion, both DNA microarray and qRT-PCR expression analyses showed that
400 transcript levels of *WSR1, 2* and *3* increased while *WSR4* decreased in ISX-treated seedlings
401 over time. *WSR* transcript levels seem to be influenced to different degrees by changes in THE1
402 activity with increased THE1 activity affecting all WSR genes while decreased THE1 activity
403 seems to affect particularly strongly *WSR1*.
404
405 **Identification of knockout and knockdown alleles for *WSR* genes**
406 Using knockout (KO) or knockdown (KD) alleles generated through T-DNA
407 insertions is a well-established and successful method to characterize genes of interest (Alonso
408 et al., 2003). We identified two independent T-DNA insertion lines for each of the four genes
409 using the Arabidopsis Gene Mapping Tool (http://signal.salk.edu/cgi-bin/tdnaexpress). Plants
410 homozygous for the insertions were isolated using PCR-based genotyping as well as insertion
411 positions in the individual gene and their effects on transcript levels determined. For *WSR1* the
412 first insertion is located in the 5' (*wsr1-1,* Salk_046217) and the second (*wsr1-2,* Salk_092919)
413 in the 3' untranslated region of the gene (Figure S4a). The insertions in *WSR2* were mapped to
414 the first intron (*wsr2-2,* Salk_123509) and the third exon (*wsr2-1,* Salk_058271) (Figure S4b).
415 For *WSR3* the insertions were located either in the promoter region (*wsr3-2*, SALK_079548) or
416 in the 10th intron (*wsr3-1*, SALK_039575) (Figure S4c). In the *wsr4-2* (SALK_121365) allele
417 the insertion is located in the 1st while the one giving rise to the *wsr4-1* (SALK_082484) allele

418 is located in the 2nd exon (Figure S4d). To determine if the insertions affect transcript levels of
419 the genes, we performed qRT-PCR using total RNA isolated from mock-treated 7 days-old
420 seedlings. These experiments identified four bona fide KO- (*wsr2-1*, *wsr2-2*, *wsr3-1*, *wsr4-2*)
421 and four KD-alleles (*wsr1-1*, *wsr1-2*, *wsr3-2* and *wsr4-1*) for the candidate genes (Figure S4a-
422 d).
423

424 **Responses to ISX-induced CWD are modified in seedlings with insertions in *WSR1* or *4***

425 ISX-induced CWD leads to lignin deposition in seedling root tips as well as increased
426 JA and SA production (Cano-Delgado et al., 2003; Ellis & Turner, 2001; Hamann et al., 2009).
427 Here we investigated if the KO / KD alleles isolated for the candidate genes affect these
428 responses by performing experiments with mock or ISX-treated seedlings in liquid culture.
429 After treating the seedlings for seven hours we measured both JA and SA levels (Figure 3a, b).
430 In ISX-treated *wsr4-2* seedlings, we detected reduced production of JA while SA levels were
431 lower in *wsr1-2* seedlings. Lignin was detected after 24 h of ISX treatment using phloroglucinol
432 and quantified using image analysis (Engelsdorf et al., 2018). Mock-treated seedling roots did
433 not show any lignin deposition (Figure 4, Figure S5). We only detected a significant reduction
434 in ISX-treated *wsr4-2* seedlings in lignification after ISX-treatment. These results suggested
435 that *WSR1* and *4* might be involved in the response to ISX-induced CWD.
436

437 ***WSR1*, *2, 3* and *4* contribute to cell wall formation during stem growth**

438 To determine whether the genes of interest affect cell wall metabolism in general, the
439 levels of cellulose, uronic acids and neutral cell wall sugars were determined in cell wall
440 preparations from rosette leaves and mature stems of Col-0 and *wsr* mutant plants. Here we
441 only investigated the strongest KO or KD allele for each candidate gene. We detected a
442 reduction in cellulose content only in leaves of *wsr4-2* plants compared to Col-0 (Figure 5a).
443 Our quantification of cellulose in mature stems detected increased amounts in *wsr1-2* and *wsr2-*

444 *1*, while cellulose was reduced in *wsr4-2* stems (Figure 5b). Analysis of lignin content in stems
445 of adult plants did not detect any differences between Col-0 and mutant plants (Figure S6).
446 Analysis of neutral cell wall sugars and uronic acids in leaves detected only for the low-
447 abundant glucuronic acid in *wsr1-2* significant differences to Col-0 controls (Figure 6a). In
448 stem-derived material, we observed enhanced levels of rhamnose and xylose in *wsr1-2* (Figure
449 6b). In *wsr3-1* stems fucose, rhamnose, arabinose and galactose contents were elevated. In
450 *wsr4-2* glucose amounts were reduced while mannose was slightly enhanced compared to Col-
451 0 controls. To summarize, our cell wall analyses detected differences in cellulose and different
452 neutral cell wall sugar contents with effects detected most pronounced in stems. The similarities
453 and variability observed regarding cell wall phenotypes suggest that the different genes may be
454 involved in distinct but also overlapping aspects of cell wall metabolism in adult plants.
455
456 **Plants with insertions in *WSR1* exhibit pathogen response phenotypes**
457 It has been shown previously that the CWI monitoring RLKs *THE1* and *MIK2* affect
458 pathogen susceptibility (Van der Does et al., 2017). Here we investigated if the mutations in
459 WSR genes also affect the outcome of plant-pathogen interactions by inoculating adult plants
460 carrying insertions in the four genes with the necrotrophic fungus *Plectosphaerella cucumerina*
461 BMM (*Pc*BMM) and quantifying fungal biomass five days post inoculation (Figure 7).
462 *Arabidopsis Gβ 1* (*agb1-1*) and *irregular xylem 1* (*irx1-6*) plants were included as controls since
463 they exhibit reduced (*agb1-1*) or enhanced resistance (*irx1-6*) to *Pc*BMM infection (Hernandez-
464 Blanco et al., 2007; Llorente et al., 2005). Fungal growth on infected *wsr2-1*, *3-1* and *4-2* plants
465 was similar to Col-0 controls. However, growth was significantly enhanced on *wsr1-2* plants,
466 suggesting that reduction of *WSR1* gene expression affects resistance to *Pc*BMM infection and
467 implicating this gene in disease resistance response.
468

Discussion

In plants a mechanism is existing, which monitors and maintains the functional integrity of the cell walls (Doblas et al., 2018; Wolf, 2017). This mechanism seems to exhibit similarities to the one described in *S. cerevisiae* and is capable of detecting CWD and initiating adaptive changes in cellular and cell wall metabolism to maintain the functional integrity of the wall (Hamann, 2015). Understanding of the molecular mechanisms underlying CWD perception and the signaling cascades involved in regulating the CWD response in plants is increasing (Engelsdorf et al., 2018; Feng et al., 2018). However, our knowledge of the genes and molecular processes bringing about changes in cell wall metabolism in response to CWD and their function during growth and development is very limited. Here, we have determined if we can identify genes mediating responses to CWD in seedlings and cell wall metabolism in adult plants by combining seedling-derived transcriptomics data with FTIR-based cell wall analysis of seedlings with T-DNA insertions in selected candidate genes. This approach identified 14 genes (out of 23 original candidates), whose functions are not well understood and which belong to different gene families (Table S1). Very little is known about the biological function of *At1g74440* beyond that it encodes an ER membrane protein. The gene has been implicated in biotic and abiotic stress responses mediated by Plant Natriuretic Peptides (PNPs) based on co-expression with *AtPNP-A* (Meier et al., 2008). *ATFIM2* encodes a protein belonging to the Fimbrin family and seems to modulates the organization of actin filaments (Zhang et al., 2016). *SQE2* encodes a squalene epoxidase converting squalene into oxidosqualene, which forms the precursor of all known angiosperm cyclic triterpenoids (Rasbery et al., 2007). Triterpenoids are required for production of membrane sterols and brassinosteroids. *PSAT1* encodes an amino transferase required for Serine biosynthesis taking place in the chloroplast (Wulfert & Krueger, 2018). Serine biosynthesis in turn is required during photorespiration, a prerequisite for carbohydrate metabolism and plant growth. While AGPs have been implicated in cell wall remodeling, very little information is available regarding the specific function of AGP7 in this

context (Seifert, 2018). *AtBXL1* encodes an enzyme acting during vascular differentiation as a β-D-xylosidase while acting as an α-L-arabinofuranosidase during seed coat development (Arsovski et al., 2009). *PRX47* encodes a putative peroxidase, is apparently expressed in differentiating vascular tissue in seedling roots and stems and involved in lignification (Tokunaga et al., 2009). *UGT71C3* and *UGT76B1* encode UDP-glycosyltransferases (UGTs), which have been implicated in glycosylation of phytohormones and / or metabolites during the response to biotic and abiotic stress (Rehman et al., 2018). UGT76B1 in particular seems to glycosylate isoleucic acid, which is required for coordination of SA- and JA-based defence responses active during infection by pathogens like *Pseudomonas syringae* and *Alternaria brassicicola* (Maksym et al., 2018). *ADR1-L1* encodes a coiled-coil nucleotide-binding leucine-rich repeat protein and forms an important element of the effector-triggered immunity in plants (Bonardi et al., 2011; Dong et al., 2016). Reviewing the available knowledge provides further evidence that several of the genes (*PRX47*, *SQE2*, *ATBXL1*, *AGP7*, *PSAT1*) are probably required for processes relevant for cell wall or plasmamembrane metabolism. Intriguingly *UGT76B1*, *UGT71C3*, *ADR1-L1* have been implicated before in the responses to abiotic or biotic stress, which also involves plant cell walls (Bonardi et al., 2011; Maksym et al., 2018; Rehman et al., 2018). In our experimental conditions the seedlings are exposed to CWD but not biotic / abiotic stress. Thus raising the possibility that these genes are actually responding to cell wall-related events, which may also occur during biotic and abiotic. More importantly the results suggest that the approach pursued here enables us to identify amongst the many genes in the Arabidopsis genome those that contribute to the responses to CWD and regulation of relevant aspects of cell wall and membrane metabolism.

We characterized four candidate genes in more detail. These had been selected based on the FTIR phenotypes apparently caused by insertions in the candidate genes and the limited detailed knowledge regarding their biological functions. qRT-PCR-based expression analysis of the four genes in ISX-treated seedlings yielded results similar to the data from the

transcriptomics experiment. Experiments with loss- and gain-of-function alleles of THE1 showed that ISX-induced changes in the transcript levels of *WSR1, 2, 3* and *4* are sensitive to an increase in the activity of THE1 (*the1-4*) while effects of reductions (*the1-1*) are less pronounced (Merz et al., 2017). These results are to be expected since complete loss of THE1 results in reduced responses to CWD but not complete losses, suggesting that the THE1-mediated CWI maintenance mechanism is either redundantly organized or other signaling mechanisms exist (Engelsdorf et al., 2018). However, the results support the notion that *WSR* gene expression is regulated by the THE1-mediated CWI maintenance mechanism and that *WSR* activity might be controlled on the transcriptional level.

Table 2 provides a global overview of the phenotypes observed for the insertion lines in the four genes. Reduction of *WSR1* and *WSR2* activity seemed to cause similarly pronounced FTIR phenotypes in an area where diagnostic signals for cellulose and pectins are normally found (Figure 1). For *wsr1-2*, we detected increased amounts of cellulose, rhamnose and xylose in stem-derived material while glucuronic acid was reduced in leaf material (Figures 5, 6). ISX-induced SA production in seedlings and resistance to *Pc*BMM in adult plants were reduced (Figures 3, 7). In *wsr2-1* plants, we also detected an increase in cellulose in stem-derived material while responses to CWD, *Pc*BMM susceptibility and non-cellulosic cell wall matrix composition were similar to the controls (Figures 3, 5, 6, 7). Reductions in *WSR3* and *4* expression seemed to result in FTIR phenotypes related to cellulose elements, hemicelluloses and pectins (Figure 1). In *wsr3-1* stem-derived cell wall material, we detected significant differences in the amounts of fucose, rhamnose, arabinose and galactose compared to controls (Figure 6). In *wsr4-2*, cellulose content was reduced both in stem- and leaf-derived cell wall material, while the amounts of glucose and mannose in stem-derived material were reduced and increased, respectively (Figure 2, 5, 6). Analysis of responses to CWD found reduced JA and lignin production in ISX-treated *wsr4-2* seedlings and no differences to wild type in *wsr3-1* seedlings (Figures 3, 4). The phenotype observed in *wsr2-1* in combination with the limited

547 available protein information provides unfortunately no new insights regarding the function of
548 WSR2 (De Abreu-Neto et al., 2013). The specific effects on neutral cell wall sugars in *wsr3-1*
549 plants suggest that WSR3 could contribute to cell wall polysaccharide metabolism possibly by
550 mediating transport between the Golgi (where non-cellulosic cell wall polysaccharides
551 containing fucose, rhamnose, arabinose, galactose are synthesized) and the plasmamembrane
552 (Temple et al., 2016). This would make sense bearing in mind that WSR3 / SFH19 belongs to
553 the SEC14-protein family, whose members have been implicated in phosphoinositide
554 production required for membrane homeostasis and signaling processes regulating cellular
555 processes like vesicle transport (Gerth et al., 2017; de Campos & Schaaf, 2017). These results
556 implicated *WSR2* and *WSR3* in cell wall metabolism but not in the representative responses to
557 CWD examined here. Both *WSR1/DIR7* and *WSR4/PXC3* seem to be required for CWD
558 responses on the seedling levels and for specific aspects of cell wall metabolism in adult plants,
559 suggesting that they are both involved in CWD-induced signaling processes regulating changes
560 in cell wall composition. *WSR1* seems only required for increased SA production in response
561 to ISX-induced CWD, whereas *WSR4* is required for both JA and lignin production. The *wsr4-*
562 *2* phenotypes were similar to those described for CWD responses in *mik2* seedlings where also
563 only JA and lignin production differ from controls while SA amounts are similar (Engelsdorf
564 et al., 2018; Van der Does et al., 2017). These results suggest that both RLKs are required for
565 the same aspects of CWI maintenance. The THE1-dependent reduction in *WSR4* transcript
566 levels in response to CWD suggest it could repress CWD-induced responses. This would be
567 similar to the CWD response phenotypes of *FER*, where a FER KD leads to enhanced
568 production of JA, SA and lignin (Engelsdorf et al., 2018). However, the *WSR4* loss of function
569 phenotypes suggest the RLK is required for ISX-induced JA and lignin production. This implies
570 the existence of additional regulatory elements interacting with WSR4 to give rise to the
571 observed mutant phenotypes. Since the related RLK PXC1 has been implicated in vascular

development a function for WSR4 in coordination of CWD perception with cell wall metabolism is conceivable (Wang et al., 2013).

To summarize, seedlings with T-DNA insertions in 14 of the 23 candidate genes that were selected in this study exhibited FTIR phenotypes. Gene expression analysis showed that *WSR* gene expression is modulated in response to ISX-induced CWD, with the modulation apparently sensitive to changes in THE1 activity. This connected the genes identified to the THE1-dependent CWI maintenance mechanism, suggesting that our approach has identified new components mediating CWI maintenance in Arabidopsis. Follow up studies with KO or KD lines for the four candidate genes found cell wall phenotypes in adult plants for all four and effects on CWD responses for *WSR1* and *4*. These results also suggest strongly that a more detailed analysis of the remaining 10 candidate genes identified, will probably yield interesting novel insights into the mode of action of the CWI maintenance mechanism and cell wall metabolism in general.

Acknowledgments

This work was supported through Gatsby AdHoc funds and a grant from the Peder Sather Center for Advanced Study to T.H. and Chris Somerville. L.K. was supported by a Ph.D. Fellowship from the Porter Institute at Imperial College and I.C. by a PhD fellowship provided by the Royal Thai government. L.D. and A.W were supported through postdoctoral fellowships provided by the Porter Institute at Imperial College. T.E. was supported through a EU Marie Curie Fellowship "SUGAROSMO-SIGNALLING" and a DFG postdoctoral fellowship (EN 1071/1-1). N.G. was supported through the EEA project grant CYTOWALL. Research by A.M. was supported by Spanish Ministry of Economy and Competitiveness (MINECO) grant BIO2015-64077-R. Programming support from Ane-Kjersti Vie and help with lignin and phytohormone quantification from Trude Johansen and the PROMEC facility at NTNU are gratefully acknowledged. The authors declare they have no conflicts of interest.

598 Alonso, J. M., Stepanova, A. N., Leisse, T. J., Kim, C. J., Chen, H., Shinn, P., Ecker, J. R.
599 (2003). Genome-wide insertional mutagenesis of Arabidopsis thaliana. *Science*,
600 *301*(5633), 653–657. https://doi.org/10.1126/science.1086391
601 Arsovski, A. A., Popma, T. M., Haughn, G. W., Carpita, N. C., McCann, M. C., & Western,
602 T. L. (2009). AtBXL1 Encodes a Bifunctional -D-Xylosidase/ -L-Arabinofuranosidase
603 Required for Pectic Arabinan Modification in Arabidopsis Mucilage Secretory Cells.
604 *Plant Physiology*, *150*(3), 1219–1234. https://doi.org/10.1104/pp.109.138388
605 Bacete, L., Mélida, H., Miedes, E., & Molina, A. (2018). Plant cell wall-mediated immunity:
606 cell wall changes trigger disease resistance responses. *Plant J*, *93*(4), 614–636.
607 https://doi.org/10.1111/tpj.13807
608 Barbosa, I. C. R., Rojas-Murcia, N., & Geldner, N. (2019). The Casparian strip—one ring to
609 bring cell biology to lignification? *Current Opinion in Biotechnology*, *56*, 121–129.
610 https://doi.org/10.1016/j.copbio.2018.10.004
611 Bidhendi, A. J., & Geitmann, A. (2015). Relating the mechanics of the primary plant cell wall
612 to morphogenesis. *Journal of Experimental Botany*, *67*(2), erv535.
613 https://doi.org/10.1093/jxb/erv535
614 Bonardi, V., Tang, S., Stallmann, A., Roberts, M., Cherkis, K., & Dangl, J. L. (2011).
615 Expanded functions for a family of plant intracellular immune receptors beyond
616 specific recognition of pathogen effectors. *Proceedings of the National Academy of*
617 *Sciences*, *108*(39), 16463–16468. https://doi.org/10.1073/pnas.1113726108
618 Cano-Delgado, A., Penfield, S., Smith, C., Catley, M., & Bevan, M. (2003). Reduced
619 cellulose synthesis invokes lignification and defense responses in Arabidopsis
620 thaliana. *Plant J*, *34*(3), 351–362. https://doi.org/1729 [pii]
621 Chang, X. F., Chandra, R., Berleth, T., & Beatson, R. P. (2008). Rapid, microscale, acetyl
622 bromide-based method for high-throughput determination of lignin content in

623 Arabidopsis thaliana. *Journal of Agricultural and Food Chemistry*, *56*(16), 6825–34.
624 https://doi.org/10.1021/jf800775f
625 Chowdhury, J., Schober, M. S., Shirley, N. J., Singh, R. R., Jacobs, A. K., Douchkov, D., &
626 Little, A. (2016). Down-regulation of the *glucan synthase-like 6* gene (*HvGsl6*) in
627 barley leads to decreased callose accumulation and increased cell wall penetration by
628 *Blumeria graminis* f. sp. *hordei*. *New Phytologist*, *212*(2), 434–443.
629 https://doi.org/10.1111/nph.14086
630 De Abreu-Neto, J. B., Turchetto-Zolet, A. C., De Oliveira, L. F. V., Bodanese Zanettini, M.
631 H., & Margis-Pinheiro, M. (2013). Heavy metal-associated isoprenylated plant protein
632 (HIPP): Characterization of a family of proteins exclusive to plants. *FEBS Journal*,
633 *280*(7), 1604–1616. https://doi.org/10.1111/febs.12159
634 De Lorenzo, G., Ferrari, S., Giovannoni, M., Mattei, B., & Cervone, F. (2018). Cell wall traits
635 that influence plant development, immunity and bioconversion. *Plant J.*
636 https://doi.org/10.1111/tpj.14196
637 Denness, L., McKenna, J. F., Segonzac, C., Wormit, A., Madhou, P., Bennett, M., & Hamann,
638 T. (2011). Cell wall damage-induced lignin biosynthesis is regulated by a reactive
639 oxygen species- and jasmonic acid-dependent process in Arabidopsis. *Plant*
640 *Physiology*, *156*(3), 1364–74. https://doi.org/10.1104/pp.111.175737
641 Dinakar, C., & Bartels, D. (2013). Desiccation tolerance in resurrection plants: new insights
642 from transcriptome, proteome and metabolome analysis. *Frontiers in Plant Science 4*,
643 482. https://doi.org/10.3389/fpls.2013.00482
644 Doblas, V. G., Gonneau, M., & Höfte, H. (2018). Cell wall integrity signaling in plants:
645 Malectin-domain kinases and lessons from other kingdoms. *The Cell Surface*, *3*, 1–11.
646 https://doi.org/10.1016/j.tcsw.2018.06.001
647 Doblas, V. G., Smakowska-luzan, E., Fujita, S., Alassimone, J., Barberon, M., Madalinski,
648 M., & Geldner, N. (2017). Root diffusion barrier control by a vasculature-derived

649 peptide binding to the SGN3 receptor, *284*, 280–284.
650 https://doi.org/10.1126/science.aaj1562
651 Doblin, M. S., Johnson, K. L., Humphries, J., Newbigin, E. J., & Bacic, A. (Tony) T. (2014).
652 Are designer plant cell walls a realistic aspiration or will the plasticity of the plant's
653 metabolism win out? *Current Opinion in Biotechnology*, *26*, 108–114.
654 https://doi.org/10.1016/j.copbio.2013.11.012
655 Dong, O. X., Tong, M., Bonardi, V., El Kasmi, F., Woloshen, V., Wünsch, L. K., & Li, X.
656 (2016). TNL-mediated immunity in *Arabidopsis* requires complex regulation of the
657 redundant *ADR1* gene family. *New Phytologist*, *210*(3), 960–973.
658 https://doi.org/10.1111/nph.13821
659 Du, S., Qu, L.-J., & Xiao, J. (2018). Crystal structures of the extracellular domains of the
660 CrRLK1L receptor-like kinases ANXUR1 and ANXUR2. *Protein Science*, *27*(4),
661 886–892. https://doi.org/10.1002/pro.3381
662 Duan, Q., Kita, D., Li, C., Cheung, A. Y., & Wu, H.-M. M. (2010). FERONIA receptor-like
663 kinase regulates RHO GTPase signaling of root hair development. *Proceedings of the*
664 *National Academy of Sciences of the United States of America*, *107*(41), 17821–
665 17826. https://doi.org/10.1073/pnas.1005366107
666 Ellis, C., & Turner, J. G. (2001). The Arabidopsis mutant cev1 has constitutively active
667 jasmonate and ethylene signal pathways and enhanced resistance to pathogens. *The*
668 *Plant Cell*, *13*(5), 1025–1033.
669 Engelsdorf, T., Gigli-Bisceglia, N., Veerabagu, M., McKenna, J. F., Vaahtera, L., Augstein,
670 F., & Hamann, T. (2018). The plant cell wall integrity maintenance and immune
671 signaling systems cooperate to control stress responses in *Arabidopsis thaliana*.
672 *Science Signaling*, *11*(536), eaao3070. https://doi.org/10.1126/scisignal.aao3070
673 Escobar-Restrepo, J.-M., Huck, N., Kessler, S., Gagliardini, V., Gheyselinck, J., Yang W. C.,
674 & Grossniklaus, U. (2007). The FERONIA receptor-like kinase mediates male-female

675 interactions during pollen tube reception. *Science*, *317*(5838), 656–660.
676 https://doi.org/317/5838/656 [pii] 10.1126/science.1143562
677 Feng, W., Kita, D., Peaucelle, A., Cartwright, H. N., Doan, V., Duan, Q., & Dinneny, J. R.
678 (2018). The FERONIA Receptor Kinase Maintains Cell-Wall Integrity during Salt
679 Stress through Ca 2+ Signaling. *Current Biology*, *28*(5), 666–675.
680 https://doi.org/10.1016/j.cub.2018.01.023
681 Franck, C. M., Westermann, J., & Boisson-Dernier, A. (2018). Plant Malectin-Like Receptor
682 Kinases: From Cell Wall Integrity to Immunity and Beyond. *Annual Review of Plant*
683 *Biology*, *69*(1), 301–328. https://doi.org/10.1146/annurev-arplant-042817-040557
684 Gerth, K., Lin, F., Menzel, W., Krishnamoorthy, P., Stenzel, I., Heilmann, M., & Heilmann, I.
685 (2017). Guilt by Association: A Phenotype-Based View of the Plant Phosphoinositide
686 Network. *Annual Review of Plant Biology*, *68*(1), 349–374.
687 https://doi.org/10.1146/annurev-arplant-042916-041022
688 Gigli-Bisceglia, N., Engelsdorf, T., Strnad, M., Vaahtera, L., Khan, G. A., Yamoune, A., &
689 Hamann, T. (2018). Cell wall integrity modulates *Arabidopsis thaliana* cell cycle gene
690 expression in a cytokinin- and nitrate reductase-dependent manner. *Development*,
691 *145*(19), dev166678. https://doi.org/10.1242/dev.166678
692 Gonneau, M., Desprez, T., Martin, M., Doblas, V. G., Bacete, L., Miart, F., & Höfte, H.
693 (2018). Receptor Kinase THESEUS1 Is a Rapid Alkalinization Factor 34 Receptor in
694 Arabidopsis. *Current Biology*, *28*(15), 2452–2458.
695 https://doi.org/10.1016/j.cub.2018.05.075
696 Guo, H., Nolan, T. M., Song, G., Liu, S., Xie, Z., Chen, J., & Yin, Y. (2018). FERONIA
697 Receptor Kinase Contributes to Plant Immunity by Suppressing Jasmonic Acid
698 Signaling in Arabidopsis thaliana. *Current Biology*, 28(20): 3316-3324
699 https://doi.org/10.1016/j.cub.2018.07.078

700 Gutierrez, R., Lindeboom, J. J., Paredez, A. R., Emons, A. M., & Ehrhardt, D. W. (2009).
701 Arabidopsis cortical microtubules position cellulose synthase delivery to the plasma
702 membrane and interact with cellulose synthase trafficking compartments. *Nat Cell*
703 *Biol*, *11*(7), 797–806. https://doi.org/ncb1886 [pii] 10.1038/ncb1886
704 Hamann, T, Bennett, M., Mansfield, J., & Somerville, C. (2009). Identification of cell-wall
705 stress as a hexose-dependent and osmosensitive regulator of plant responses. *Plant J*,
706 *57*(6), 1015–1026. https://doi.org/TPJ3744 [pii] 10.1111/j.1365-313X.2008.03744.x
707 Hamann, Thorsten. (2015). The plant cell wall integrity maintenance mechanism-concepts for
708 organization and mode of action. *Plant & Cell Physiology*, *56*(2), 215–23.
709 https://doi.org/10.1093/pcp/pcu164
710 Han, J.-P., Köster, P., Drerup, M. M., Scholz, M., Li, S., Edel, K. H., & Kudla, J. (2018).
711 Fine-tuning of RBOHF activity is achieved by differential phosphorylation and Ca^{2+}
712 binding. *New Phytologist*. https://doi.org/10.1111/nph.15543
713 Harpaz-Saad, S., McFarlane, H. E., Xu, S., Divi, U. K., Forward, B., Western, T. L., &
714 Kieber, J. J. (2011). Cellulose synthesis via the FEI2 RLK/SOS5 pathway and
715 cellulose synthase 5 is required for the structure of seed coat mucilage in Arabidopsis.
716 *Plant J 68*(6), 941–53. https://doi.org/10.1111/j.1365-313X.2011.04760.x
717 Haruta, M., Sabat, G., Stecker, K., Minkoff, B. B., & Sussman, M. R. (2014). A Peptide
718 Hormone and Its Receptor Protein Kinase Regulate Plant Cell Expansion. *Science*,
719 *343*(6169), 408–411. https://doi.org/10.1126/science.1244454
720 Heim, D. R., Skomp, J. R., Tschabold, E. E., & Larrinua, I. M. (1990). Isoxaben Inhibits the
721 Synthesis of Acid Insoluble Cell Wall Materials In Arabidopsis thaliana. *Plant*
722 *Physiol*, *93*(2), 695–700.
723 Hematy, K., Sado, P. E., Van Tuinen, A., Rochange, S., Desnos, T., Balzergue, S., & Hofte,
724 H. (2007). A receptor-like kinase mediates the response of Arabidopsis cells to the

725 inhibition of cellulose synthesis. *Curr Biol*, *17*(11), 922–931. https://doi.org/S0960-
726 9822(07)01396-6 [pii] 10.1016/j.cub.2007.05.018
727 Hernandez-Blanco, C., Feng, D. X., Hu, J., Sanchez-Vallet, A., Deslandes, L., Llorente, F., &
728 Molina, A. (2007). Impairment of cellulose synthases required for Arabidopsis
729 secondary cell wall formation enhances disease resistance. *Plant Cell*, *19*(3), 890–903.
730 https://doi.org/tpc.106.048058 [pii] 10.1105/tpc.106.048058
731 Jiménez-Quesada, M. J., Traverso, J. Á., & Alché, J. de D. (2016). NADPH Oxidase-
732 Dependent Superoxide Production in Plant Reproductive Tissues. *Frontiers in Plant*
733 *Science*, *7*. https://doi.org/10.3389/fpls.2016.00359
734 Kadota, Y., Sklenar, J., Derbyshire, P., Stransfeld, L., Asai, S., Ntoukakis, V., & Zipfel, C.
735 (2014). Direct regulation of the NADPH oxidase RBOHD by the PRR-associated
736 kinase BIK1 during plant immunity. *Molecular Cell*, *54*(1), 43–55.
737 https://doi.org/10.1016/j.molcel.2014.02.021
738 Kanaoka, M. M., & Torii, K. U. (2010). FERONIA as an upstream receptor kinase for polar
739 cell growth in plants. *Proceedings of the National Academy of Sciences of the United*
740 *States of America*, *107*(41), 17461–2. https://doi.org/10.1073/pnas.1013090107
741 KF de Campos, M., & Schaaf, G. (2017). The regulation of cell polarity by lipid transfer
742 proteins of the SEC14 family. *Current Opinion in Plant Biology*, *40*, 158–168.
743 https://doi.org/10.1016/j.pbi.2017.09.007
744 Kieber, J. J., & Polko, J. (2019). The Regulation of Cellulose Biosynthesis in Plants. *The*
745 *Plant Cell*, tpc.00760.2018. https://doi.org/10.1105/tpc.18.00760
746 Lee, Y., Rubio, M. C., Alassimone, J., & Geldner, N. (2013). A mechanism for localized
747 lignin deposition in the endodermis. *Cell*, *153*(2), 402–12.
748 https://doi.org/10.1016/j.cell.2013.02.045

749 Levin, D. E. (2011). Regulation of cell wall biogenesis in Saccharomyces cerevisiae: the cell
750 wall integrity signaling pathway. *Genetics*, *189*(4), 1145–75.
751 https://doi.org/10.1534/genetics.111.128264
752 Liu, P., Haruta, M., Minkoff, B. B., & Sussman, M. R. (2018). Probing a Plant Plasma
753 Membrane Receptor Kinase's Three-Dimensional Structure Using Mass
754 Spectrometry-Based Protein Footprinting. *Biochemistry*, *57*(34), 5159–5168.
755 https://doi.org/10.1021/acs.biochem.8b00471
756 Llorente, F., Alonso-Blanco, C., Sanchez-Rodriguez, C., Jorda, L., & Molina, A. (2005).
757 ERECTA receptor-like kinase and heterotrimeric G protein from Arabidopsis are
758 required for resistance to the necrotrophic fungus Plectosphaerella cucumerina. *Plant*
759 *J*, *43*(2), 165–180. https://doi.org/10.1111/j.1365-313X.2005.02440.x
760 Maksym, R. P., Ghirardo, A., Zhang, W., von Saint Paul, V., Lange, B., Geist, B., &
761 Schäffner, A. R. (2018). The Defense-Related Isoleucic Acid Differentially
762 Accumulates in Arabidopsis Among Branched-Chain Amino Acid-Related 2-Hydroxy
763 Carboxylic Acids. *Frontiers in Plant Science*, *9*.
764 https://doi.org/10.3389/fpls.2018.00766
765 Manfield, I. W., Orfila, C., Mccartney, L., Harholt, J., Bernal, A. J., Scheller, H. V., &
766 Willats, W. G. T. (2004). Novel cell wall architecture of isoxaben-habituated
767 Arabidopsis suspension-cultured cells: global transcript profiling and cellular analysis.
768 *Plant J*, *40*(2), 260–275. https://doi.org/10.1111/j.1365-313X.2004.02208.x
769 Meier, S., Bastian, R., Donaldson, L., Murray, S., Bajic, V., & Gehring, C. (2008). Co-
770 expression and promoter content analyses assign a role in biotic and abiotic stress
771 responses to plant natriuretic peptides. *BMC Plant Biology*, *8*(1), 24.
772 https://doi.org/10.1186/1471-2229-8-24
773 Merz, D., Richter, J., Gonneau, M., Sanchez-Rodriguez, C., Eder, T., Sormani, R., & Hauser,
774 M.-T. (2017). T-DNA alleles of the receptor kinase THESEUS1 with opposing effects

775 on cell wall integrity signaling. *Journal of Experimental Botany*, *68*(16), 4583–4593.
776 https://doi.org/10.1093/jxb/erx263
777 Mouille, G., Robin, S., Lecomte, M., Pagant, S., & Hofte, H. (2003). Classification and
778 identification of Arabidopsis cell wall mutants using Fourier-Transform InfraRed (FT-
779 IR) microspectroscopy. *Plant J*, *35*(3), 393–404.
780 Moussu, S., Augustin, S., Roman, A.-O., Broyart, C., & Santiago, J. (2018). Crystal structures
781 of two tandem malectin-like receptor kinases involved in plant reproduction. *Acta*
782 *Crystallographica Section D Structural Biology*, *74*(7), 671–680.
783 https://doi.org/10.1107/S205979831800774X
784 Nakagawa, Y., Katagiri, T., Shinozaki, K., Qi, Z., Tatsumi, H., Furuichi, T., & Iida, H.
785 (2007). Arabidopsis plasma membrane protein crucial for Ca2+ influx and touch
786 sensing in roots. *Proc Natl Acad Sci U S A*, *104*(9), 3639–3644.
787 https://doi.org/0607703104 [pii] 10.1073/pnas.0607703104
788 Novaković L. , Guo T., Bacic A., Sampathkumar A. & Johnson KL . (2018) Hitting the Wall-
789 Sensing and Signalling Pathways Involved in Plant Cell Wall Remodeling in Response
790 to Abiotic Stress. *Plants* 23;7(4). [pii]: E89. doi: 10.3390/plants7040089.
791 Paniagua, C., Bilkova, A., Jackson, P., Dabravolski, S., Riber, W., Didi, V., & Hejatko, J.
792 (2017). Dirigent proteins in plants: modulating cell wall metabolism during abiotic
793 and biotic stress exposure. *Journal of Experimental Botany*, *68*(13), 3287–3301.
794 https://doi.org/10.1093/jxb/erx141
795 Paredez, A. R., Somerville, C. R., & Ehrhardt, D. W. (2006). Visualization of cellulose
796 synthase demonstrates functional association with microtubules. *Science*, *312*(5779),
797 1491–1495. https://doi.org/1126551 [pii] 10.1126/science.1126551
798 Rasbery, J. M., Shan, H., LeClair, R. J., Norman, M., Matsuda, S. P., & Bartel, B. (2007).
799 Arabidopsis thaliana squalene epoxidase 1 is essential for root and seed development.

The Journal of Biological Chemistry, *282*(23), 17002–17013. https://doi.org/10.1074/jbc.M611831200

Rehman, H. M., Nawaz, M. A., Shah, Z. H., Ludwig-Müller, J., Chung, G., Ahmad, M. Q., & Lee, S. I. (2018). Comparative genomic and transcriptomic analyses of Family-1 UDP glycosyltransferase in three Brassica species and Arabidopsis indicates stress-responsive regulation. *Scientific Reports*, *8*(1). https://doi.org/10.1038/s41598-018-19535-3

Scheible, W. R., Eshed, R., Richmond, T., Delmer, D., & Somerville, C. (2001). Modifications of cellulose synthase confer resistance to isoxaben and thiazolidinone herbicides in Arabidopsis Ixr1 mutants. *Proc Natl Acad Sci U S A*, *98*(18), 10079–10084. https://doi.org/10.1073/pnas.191361598 191361598 [pii]

Seifert, G. (2018). Fascinating Fasciclins: A Surprisingly Widespread Family of Proteins that Mediate Interactions between the Cell Exterior and the Cell Surface. *International Journal of Molecular Sciences*, *19*(6), 1628. https://doi.org/10.3390/ijms19061628

Shi, H., Kim, Y., Guo, Y., Stevenson, B., & Zhu, J. K. (2003). The Arabidopsis SOS5 locus encodes a putative cell surface adhesion protein and is required for normal cell expansion. *The Plant Cell*, *15*(1), 19–32.

Shih, H. W., Miller, N. N. D. D., Dai, C., Spalding, E. E. P. P., & Monshausen, G. B. B. G. (2014). The Receptor-like Kinase FERONIA Is Required for Mechanical Signal Transduction in Arabidopsis Seedlings. *Current Biology*, *24*(16), 1887–1892. https://doi.org/10.1016/j.cub.2014.06.064

Stegmann, M., Monaghan, J., Smakowska-Luzan, E., Rovenich, H., Lehner, A., Holton, N., & Zipfel, C. (2017). The receptor kinase FER is a RALF-regulated scaffold controlling plant immune signaling. *Science*, *355*, 287–289. https://doi.org/10.1126/science.aal2541

825 Szymanska-Chargot, M., Chylinska, M., Kruk, B., & Zdunek, A. (2015). Combining FT-IR
826 spectroscopy and multivariate analysis for qualitative and quantitative analysis of the
827 cell wall composition changes during apples development. *Carbohydrate Polymers*,
828 *115*, 93–103. https://doi.org/10.1016/j.carbpol.2014.08.039
829 Tateno, M., Brabham, C., & DeBolt, S. (2016). Cellulose biosynthesis inhibitors – a
830 multifunctional toolbox. *Journal of Experimental Botany*, *67*(2), 533–542.
831 https://doi.org/10.1093/jxb/erv489
832 Temple, H., Saez-Aguayo, S., Reyes, F. C., & Orellana, A. (2016). The inside and outside:
833 topological issues in plant cell wall biosynthesis and the roles of nucleotide sugar
834 transporters. *Glycobiology*, *26*(9), 913–925. https://doi.org/10.1093/glycob/cww054
835 Tokunaga, N., Kaneta, T., Sato, S., & Sato, Y. (2009). Analysis of expression profiles of three
836 peroxidase genes associated with lignification in Arabidopsis thaliana. *Physiologia*
837 *Plantarum*, *136*(2), 237–249. https://doi.org/10.1111/j.1399-3054.2009.01233.x
838 Van der Does, D., Boutrot, F., Engelsdorf, T., Rhodes, J., McKenna, J. F., Vernhettes, S., &
839 Zipfel, C. (2017). The Arabidopsis leucine-rich repeat receptor kinase MIK2/LRR-
840 KISS connects cell wall integrity sensing, root growth and response to abiotic and
841 biotic stresses. *PLOS Genetics*, *13*(6), e1006832.
842 https://doi.org/10.1371/journal.pgen.1006832
843 Wang, J., Kucukoglu, M., Zhang, L., Chen, P., Decker, D., Nilsson, O., & Zheng, B. (2013).
844 The Arabidopsis LRR-RLK, PXC1, is a regulator of secondary wall formation
845 correlated with the TDIF-PXY/TDR-WOX4 signaling pathway. *BMC Plant Biology*,
846 *13*(1), 1–11. https://doi.org/10.1186/1471-2229-13-94
847 Wilson, R. H., Smith, A. C., Kacurakova, M., Saunders, P. K., Wellner, N., & Waldron, K.
848 W. (2000). The mechanical properties and molecular dynamics of plant cell wall
849 polysaccharides studied by Fourier-transform infrared spectroscopy. *Plant Physiol*,
850 *124*(1), 397–405.

851 Wolf, S. (2017). Plant cell wall signaling and receptor-like kinases. *Biochemical Journal*,
852 *474*(4), 471–492. https://doi.org/10.1042/BCJ20160238
853 Wuest, S. E., Vijverberg, K., Schmidt, A., Weiss, M., Gheyselinck, J., Lohr, M., &
854 Grossniklaus, U. (2010). Arabidopsis female gametophyte gene expression map
855 reveals similarities between plant and animal gametes. *Current Biology: CB*, *20*(6),
856 506–512. https://doi.org/10.1016/j.cub.2010.01.051
857 Wulfert, S., & Krueger, S. (2018). Phosphoserine Aminotransferase1 Is Part of the
858 Phosphorylated Pathways for Serine Biosynthesis and Essential for Light and Sugar-
859 Dependent Growth Promotion. *Frontiers in Plant Science*, *9*.
860 https://doi.org/10.3389/fpls.2018.01712
861 Xu, S.-L. L., Rahman, A., Baskin, T. I., & Kieber, J. J. (2008). Two leucine-rich repeat
862 receptor kinases mediate signaling, linking cell wall biosynthesis and ACC synthase in
863 Arabidopsis. *The Plant Cell*, *20*(11), 3065–3079. https://doi.org/tpc.108.063354 [pii]
864 10.1105/tpc.108.063354
865 Xue, H., Veit, C., Abas, L., Tryfona, T., Maresch, D., Ricardi, M. M., & Seifert, G. J. (2017).
866 *Arabidopsis thaliana FLA4* functions as a glycan-stabilized soluble factor via its
867 carboxy-proximal Fasciclin 1 domain. *Plant J*, *91*(4), 613–630.
868 https://doi.org/10.1111/tpj.13591
869 Yeats, T., Vellosillo, T., Sorek, N., Ibáñez, A. B., & Bauer, S. (2016). Rapid Determination of
870 Cellulose, Neutral Sugars, and Uronic Acids from Plant Cell Walls by One-step Two-
871 step Hydrolysis and HPAEC-PAD. *Bio-Protocol*, *6*(20), e1978.
872 https://doi.org/10.21769/BioProtoc.1978
873 Yu, F., Qian, L., Nibau, C., Duan, Q., Kita, D., Levasseur, K., & Luan, S. (2012). FERONIA
874 receptor kinase pathway suppresses abscisic acid signaling in Arabidopsis by
875 activating ABI2 phosphatase. *Proceedings of the National Academy of Sciences of the*
876 *United States of America*, *109*(36), 14693–8. https://doi.org/10.1073/pnas.1212547109

877 Zhang, R., Chang, M., Zhang, M., Wu, Y., Qu, X., & Huang, S. (2016). The Structurally
878 Plastic CH2 Domain Is Linked to Distinct Functions of Fimbrins/Plastins. *Journal of*
879 *Biological Chemistry*, *291*(34), 17881–17896.
880 https://doi.org/10.1074/jbc.M116.730069
881 Zhao, F., Chen, W., & Traas, J. (2018). ScienceDirect Mechanical signaling in plant
882 morphogenesis. *Current Opinion in Genetics & Development*, *51*, 26–30.
883 https://doi.org/10.1016/j.gde.2018.04.001
884

885 **Table 1:** Candidate genes selected from the transcriptomics / FTIR- based screen. Gene
886 annotations are based on Araport11 and references listed. WSR: Wall Stress Response.
887
888
889
890
891
892
893
894

	AGI	Gene Annotation	Reference
WSR1	*At3g13650*	*DIR7*, Disease resistance-responsive (dirigent-like protein) family protein	Paniagua et al., 2017
WSR2	*At2g35730*	Heavy metal transport / detoxification superfamily protein	De Abreu-Neto et al., 2013
WSR3	*At5g47730*	*SFH19*, Sec14p-like phosphatidylinositol transfer family protein	De Campos et al., 2017
WSR4	*At2g41820*	*PXC3*, Leucine-rich repeat protein kinase family protein	Wang et al., 2013

Table 2: Overview of the phenotypes observed for mutant lines of the different candidate genes examined. Statistically significant differences compared to the wild type are indicated with blue (increased) or red (decreased) arrows.

		wsr1	*wsr2*	*wsr3*	*wsr4*
Cell wall damage response (6 day-old seedlings)	JA	-	-	-	↓
	SA	↓	-	-	-
	Lignin	-	-	-	↓
Cell wall composition (5 week-old plants)	Cellulose	stem ↑	stem ↑	-	leaf ↓ stem ↓
	Fucose	-	-	stem ↑	-
	Rhamnose	stem ↑	-	stem ↑	-
	Arabinose	-	-	stem ↑	-
	Galactose	-	-	stem ↑	-
	Glucose	-	-	-	stem ↓
	Xylose	stem ↑	-	-	-
	Mannose	-	-	-	stem ↑
	Galacturonic acid	-	-	-	-
	Glucuronic acid	leaf ↓	-	-	-
PcBMM susceptibility (18 day-old plants)		↑	-	-	-

900 **Figure legends**

901 **Figure 1. Overview of average Fourier-Transform Infrared (FTIR) spectra from Col-0,**
902 ***wsr1-1, wsr2-1, wsr3-1* and *wsr4-1* seedlings.** Black lines indicate 2 x SD for Col-0-derived
903 material. The differently coloured lines for *wsr1-1* (*DIR7*), *wsr2-1* (*At3g35730*), *wsr3-1*
904 (*SFH19*) and *wsr4-1* (*PXC3*) are based on the normalized average FTIR spectra for Col-0
905 seedlings minus the average spectra of the individual mutant. Numbers in red indicate bands in
906 the infrared spectra of plant cell wall material indicative for certain classes of cell wall
907 polysaccharides.

908

909 **Figure 2. Candidate gene expression profiling in seedlings exposed to cellulose**
910 **biosynthesis inhibition.**
911 **(a)** Gene expression of *WSR1*, *2*, *3* and *4* in Col-0 seedlings at the indicated time points after
912 mock (empty symbols, dotted lines) or ISX (filled symbols, solid lines) treatment according to
913 qRT-PCR analysis. Values were normalized to *ACT2* and represent means from 3
914 independent experiments (n=9). Error bars indicate SD. Asterisks indicate statistically
915 significant differences (*$p < 0.05$) to mock controls according to Student‘s t test. (**b**)
916 Transcript levels of *WSR1*, *2*, *3* and *4* in Col-0, *the1-1* and *the1-4* seedlings mock (DMSO) or
917 ISX-treated for 8 hours. Values were normalized to *ACT2* and represent means from 3
918 independent experiments (n= 8-9). Asterisks indicate statistically significant differences to
919 mock controls according to Student‘s t test (*$p < 0.05$). The boxes in the boxplot indicate
920 interquartile range (IQR, between 25th and 75th percentile) and the black line in the middle of
921 the box marks the median. The whiskers indicate data points furthest from the median, if they
922 are still within 1.5xIQR from the closest quartile. The data points outside this range are
923 plotted individually.

924

925 **Figure 3. Relative jasmonic acid and salicylic acid accumulation in *wsr* seedlings after ISX**
926 **treatment.**
927 **(a)** Jasmonic acid and **(b)** salicylic acid were quantified in Col-0, *wsr1-1*, *wsr1-2*, *wsr2-1*, *wsr2-*
928 *2*, *wsr3-1, wsr3-2*, *wsr4-1* and *wsr4-2* seedlings after 7 h of mock (empty bars) or ISX (filled
929 bars) treatment. Bars represent mean values from 3-4 independent experiments and error bars
930 indicate SD. Asterisks indicate statistically significant differences to the ISX-treated wild type
931 according to Student‘s t test (*$p < 0.05$).
932
933 **Figure 4. Relative lignification in *wsr* root tips after ISX treatment.**
934 Lignification in root tips of Col-0, *wsr1-1*, *wsr1-2*, *wsr2-1*, *wsr2-2*, *wsr3-1, wsr3-2*, *wsr4-1* and
935 *wsr4-2* seedlings was quantified after 24 h of ISX treatment. Bars represent mean values from
936 3 independent experiments and error bars indicate SD. Asterisks indicate statistically significant
937 differences to the wild type according to Student‘s t test (*$p < 0.05$).
938
939 **Figure 5. Cellulose content in adult *wsr* plants.**
940 Cellulose content was quantified in cell wall preparations from 5 weeks-old Col-0, *wsr1-2*,
941 *wsr2-1*, *wsr3-1* and *wsr4-2* plants. **(a)** Leaf cellulose, **(b)** stem cellulose. Bars represent mean
942 values and error bars indicate SD ($n = 4$). Asterisks indicate statistically significant differences
943 to the wild type according to Student‘s t test (*$p < 0.05$; **$p < 0,01$).
944
945 **Figure 6. Cell wall matrix monosaccharide composition in adult *wsr* plants.** Relative
946 amounts of the monosaccharides Fucose, Rhamnose, Arabinose, Galactose, Glucose, Xylose,
947 Mannose, Galacturonic acid and Glucoronic acid were quantified in cell wall matrix
948 hydrolysates of 5 weeks-old Col-0, *wsr1-2*, *wsr2-1*, *wsr3-1* and *wsr4-2* plants. **(a)** Leaf
949 monosaccharides, **(b)** stem monosaccharides. Bars represent mean values and error bars

950 indicate SD (n = 4). Asterisks indicate statistically significant differences to the wild type
951 according to Student‘s t test (*p < 0.05; **p < 0,01).
952
953 **Figure 7 Relative susceptibility of *wsr* plants to *Plectosphaerella cucumerina*.**
954 3 weeks-old Col-0, *wsr1-2*, *wsr2-1*, *wsr3-1, wsr4-2*, *irx1-6* (resistance control) and *agb1-1*
955 (susceptibility control) plants were infected with the necrotrophic leaf pathogen isolate
956 *Plectosphaerella cucumerina* BMM (*Pc*BMM). The relative fungal biomass was determined 5
957 days post infection (dpi) by qPCR analysis of the *Pc*BMM β-tubulin gene. Bars represent mean
958 values and error bars indicate SD (n = 4-6). Asterisks indicate statistically significant
959 differences to the wild type according to Student‘s t test (*p < 0.05; **p < 0,01).

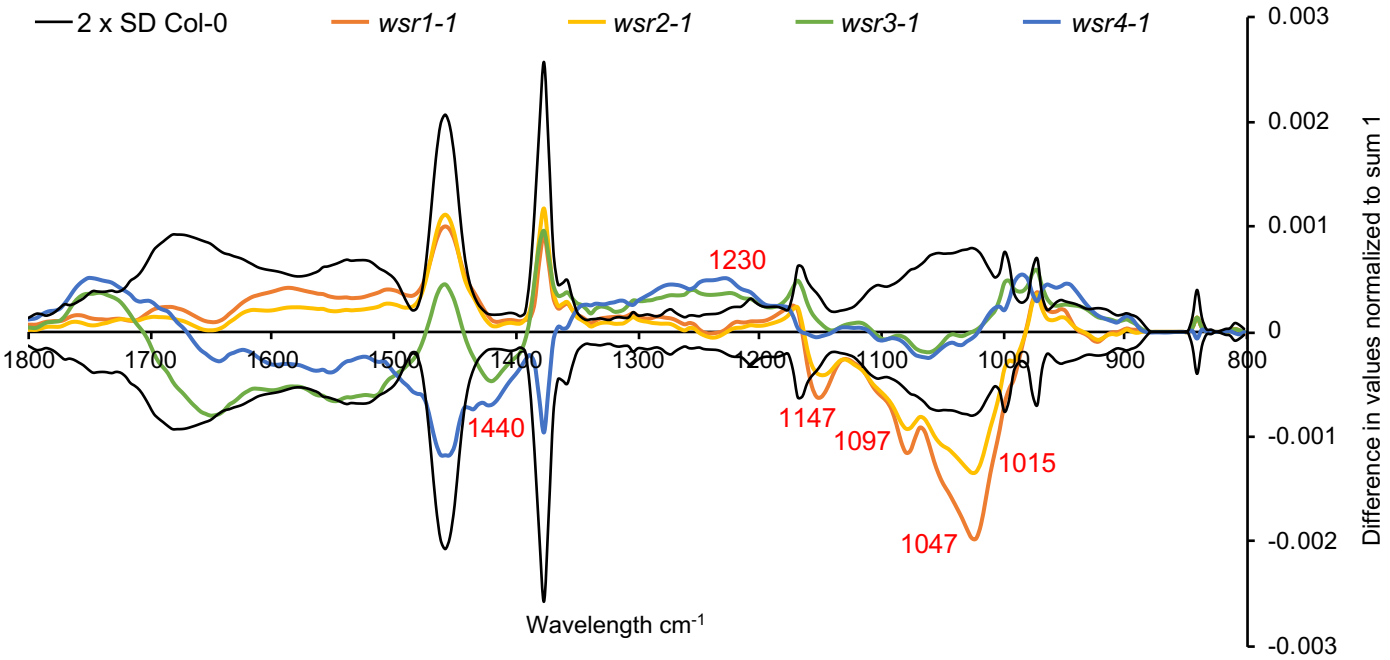

Figure 1: Overview of average Fourier-Transform Infrared (FTIR) spectra from Col-0, *wsr1-1, wsr2-1, wsr3-1* and *wsr4-1* seedlings. Black lines indicate 2 x SD for Col-0 derived material. The different colored lines for *wsr1-1* (*DIR7*), *wsr2-1* (*At3g35730*), *wsr3-1* (*SFH19*) and *wsr4-1* (*PXC3*) are based on the normalized average FTIR spectra for Col-0 seedlings minus the average spectra of the individual mutant. Numbers in red indicate bands in the infrared spectra of plant cell wall material indicative for certain classess of cell wall polysaccharides.

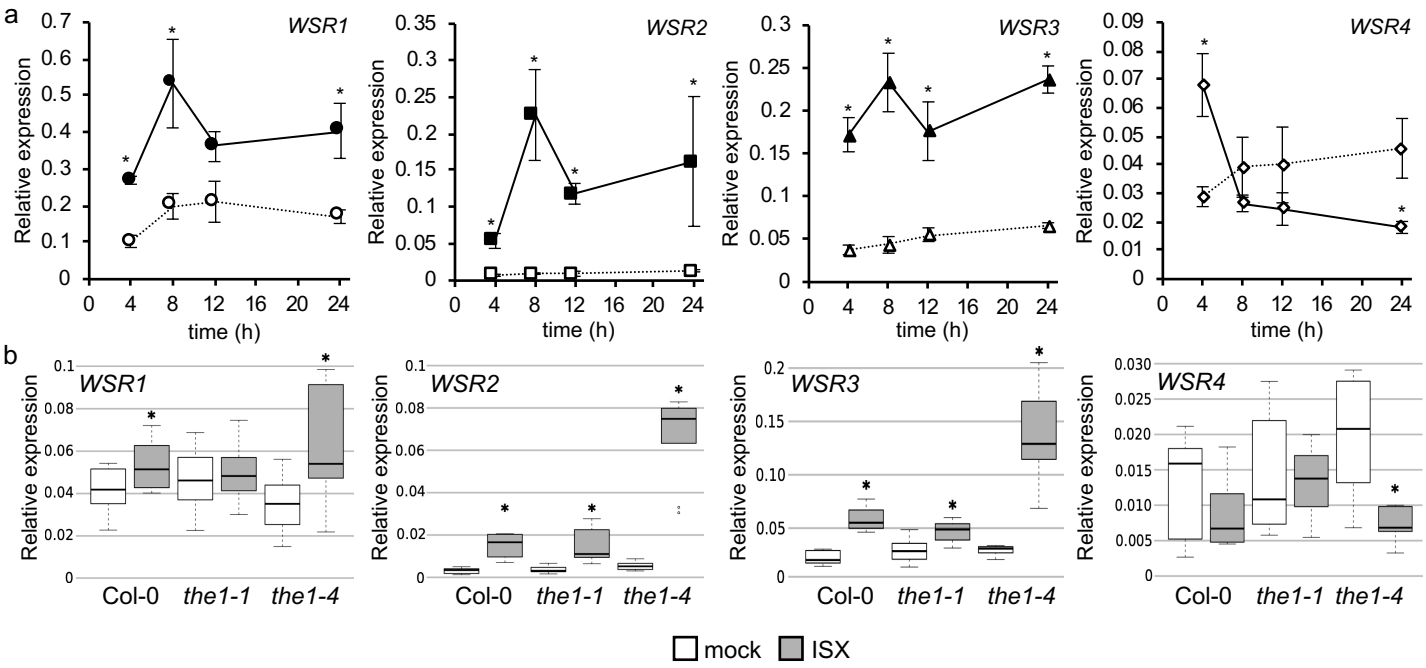

Figure 2 . Candidate gene expression profiling in seedlings exposed to cellulose biosynthesis inhibition. **(a)** Gene expression of *WSR1*, *2*, *3* and *4* in Col-0 seedlings at the indicated time points after mock (empty symbols , dotted lines) or ISX (filled symbols , solid lines) treatment according to qRT-PCR analysis. Values were normalized to *ACT2* and represent means from 3 independent experiments (n=9). Error bars indicate SD. Asterisks indicate statistically significant differences (*p < 0.05) to mock controls according to Student's t test. (**b**) Transcript levels of *WSR1*, *2*, *3* and *4* in Col-0, *the1-1* and *the1-4* seedlings mock (DMSO) or ISX-treated for 8 hours. Values were normalized to *ACT2* and represent means from 3 independent experiments (n= 8-9). Asterisks indicate statistically significant differences to mock controls according to Student's t test (*p < 0.05). The boxes in the boxplot indicate interquartile range (IQR, between 25th and 75th percentile) and the black line in the middle of the box marks the median. The whiskers indicate data points furthest from the median, if they are still within 1.5xIQR from the closest quartile. The data points outside this range are plotted individually.

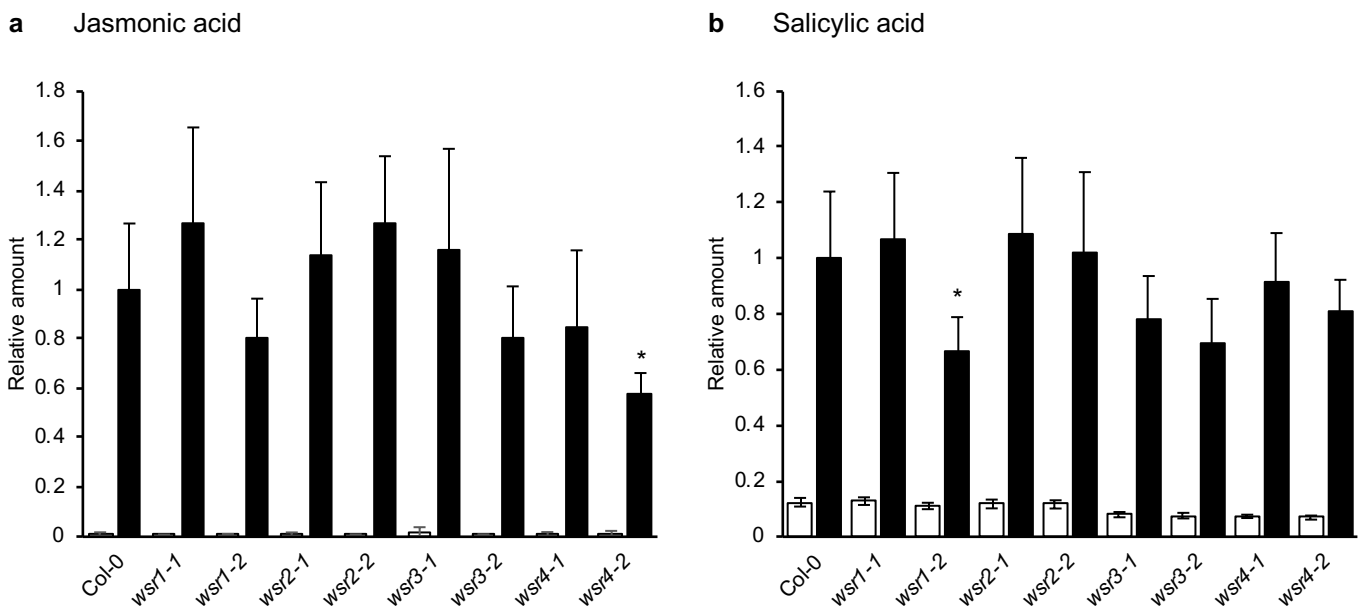

Figure 3: Relative jasmonic acid and salicylic acid accumulation in *wsr* seedlings after isoxaben treatment. (a) Jasmonic acid and **(b)** salicylic acid were quantified in Col-0, *wsr1-1*, *wsr1-2*, *wsr2-1*, *wsr2-2*, *wsr3-1, wsr3-2*, *wsr4-1* and *wsr4-2* seedlings after 7 h of mock (empty bars) or ISX (filled bars) treatment. Bars represent mean values from 3-4 independent experiments and error bars indicate SD. Asterisks indicate statistically significant differences to the ISX-treated wild type according to Student‘s t test (*$p < 0.05$).

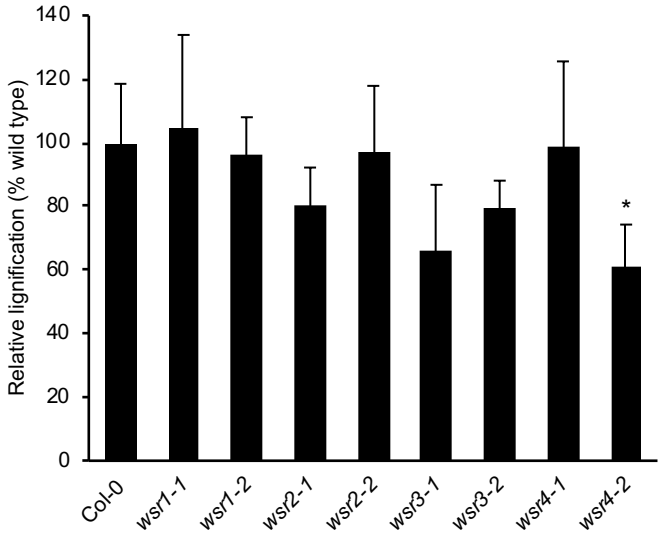

Figure 4: Relative lignification in *wsr* root tips after ISX treatment. Lignification in root tips of Col-0, *wsr1-1*, *wsr1-2*, *wsr2-1*, *wsr2-2*, *wsr3-1, wsr3-2*, *wsr4-1* and *wsr4-2* seedlings was quantified after 24 h of isoxaben treatment. Bars represent mean values from 3 independent experiments (n= 10-15) and error bars indicate SD. Asterisks indicate statistically significant differences to the wild type according to Student‘s t test (*$p < 0.05$).

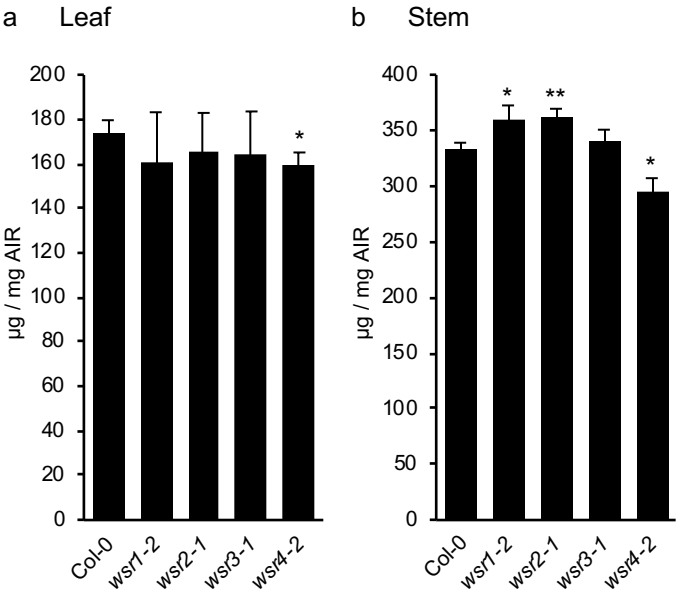

Figure 5: Cellulose content in adult *wsr* plants. Cellulose content was quantified in cell wall preparations from 5 weeks-old Col-0, *wsr1-2*, *wsr2-1*, *wsr3-1* and *wsr4-2* plants. **(a)** Leaf cellulose, **(b)** stem cellulose. Bars represent mean values and error bars indicate SD (n= 4). Asterisks indicate statistically significant differences to the wild type according to Student‘s t test (*$p < 0.05$; **$p < 0.01$).

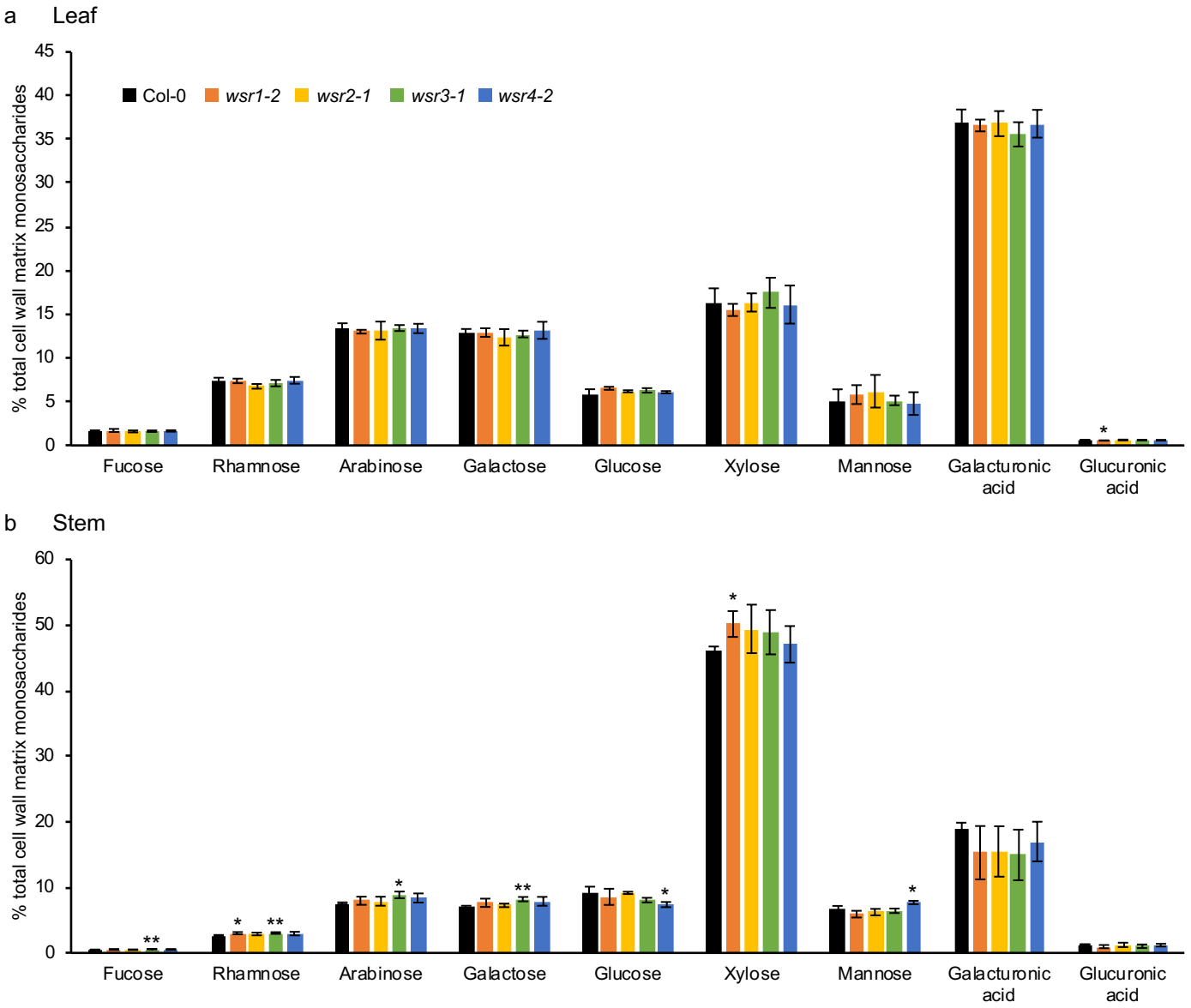

Figure 6: Cell wall matrix monosaccharide composition in adult *wsr* plants. Relative amounts of the monosaccharides Fucose, Rhamnose, Arabinose, Galactose, Glucose, Xylose, Mannose, Galacturonic acid and Glucoronic acid were quantified in cell wall matrix hydrolysates of 5 weeks-old Col-0, *wsr1-2*, *wsr2-1*, *wsr3-1* and *wsr4-2* plants. **(a)** Leaf monosaccharides, **(b)** stem monosaccharides. Bars represent mean values and error bars indicate SD (n= 4). Asterisks indicate statistically significant differences to the wild type according to Student‘s t test (*$p < 0.05$; **$p < 0.01$).

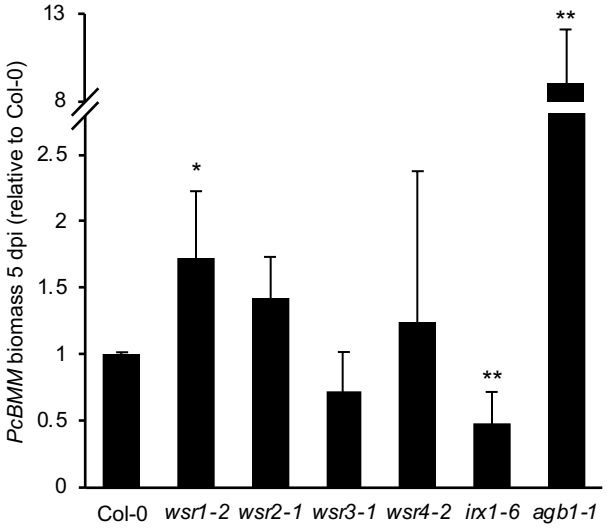

Figure 7: Relative susceptibility of *wsr* plants to *Plectosphaerella cucumerina*. 18 days-old Col-0, *wsr1-2*, *wsr2-1*, *wsr3-1, wsr4-2*, *irx1-6* (resistance control) and *agb1-1* (susceptibility control) plants were infected with the necrotrophic leaf pathogen isolate *Plectosphaerella cucumerina BMM* (*PcBMM*). The relative fungal biomass was determined 5 days post infection (dpi) by qPCR analysis of the *PcBMM* β-tubulin gene. Bars represent mean values and error bars indicate SD (n= 4-6). Asterisks indicate statistically significant differences to the wild type according to Student‘s t test (*$p < 0.05$; **$p < 0.01$).